Effect of clay type on dispersion and barrier properties of hydrophobically modified poly(vinyl alcohol)-bentonite nanocomposites

JOHANSSON, Caisa and CLEGG, Francis <http://orcid.org/0000-0002-9566-5739>

Effect of clay type on dispersion and barrier properties of hydrophobically modified poly(vinyl alcohol)-bentonite nanocomposites

Caisa Johansson[1,*] and Francis Clegg[2]

[1] Karlstad University, Faculty of Health, Science and Technology, Department of Engineering and Chemical Sciences, SE-651 88 Karlstad, Sweden. *Corresponding author. Email: caisa.johansson@kau.se, Tel +46547001606, Fax +46547002040.

[2] Materials and Engineering Research Institute, Sheffield Hallam University, Howard Street, Sheffield S1 1WB, U.K.

KEYWORDS: clay, composites, films, packaging, surfaces and interfaces

ABSTRACT

The oxygen and water vapor permeability at high relative humidity was studied for composite films formed by incorporation of three different bentonites (MMT) clays into an ethylene modified, water-soluble poly(vinyl alcohol), EPVOH. The oxygen permeability decreased linearly with increased addition of hydrophilic MMTs. X-ray diffraction and Fourier transform infrared spectroscopy suggested a homogeneous distribution in the thickness direction with disordered and probably exfoliated hydrophilic MMTs. In contrast, organophilic modified clay showed an intercalated structure with the clay preferentially located at the lower film surface, a combination which was however efficient in reducing the water vapor- and oxygen permeabilities at low addition levels. Composite films of EPVOH and Na^+-exchanged MMT resulted in a high resistance to dissolution in water, which was ascribed to strong interactions between the components due to matching polarities. Annealing the films at 120°C resulted in enhanced resistance to water dissolution and a further reduction in oxygen permeability.

INTRODUCTION

Ethylene vinyl alcohol (EVOH) copolymers are known for their outstanding gas barrier properties that are superior to other polymers conventionally used in packaging. Their highest oxygen barrier properties have been shown to occur within the range of 27-32 mol% ethylene.[1] However, the poor water solubility of EVOH copolymers at high ethylene content restrict them to use in water-free processes like extrusion coating and blow molding.[1,2] Consequently, water-soluble ethylene modified copolymers of poly(vinyl alcohol), here abbreviated to EPVOH, have recently been introduced on the market.

Conventional poly(vinyl alcohol), PVOH, films are hydrophilic and the barrier properties are thus strongly affected by the surrounding relative humidity, RH. For instance the oxygen permeability of PVOH films in general increases 2500 times when going from 0% RH to 100% RH.[3] The ethylene modification however gives the polymer a hydrophobic character and films of EPVOH are stated to have lower oxygen transmission rates (OTR) than standard PVOH films by almost an order of magnitude[4]; they are also more effective barriers at higher relative humidities.[5] These water-soluble EPVOHs are also claimed to have OTR values below that of commercial EVOH coatings (27 mol% ethylene) in the range from 0 to 70% RH.[4] Thus, the water-solubility together with favorable barrier properties and approval for food contact, give the novel EPVOH grades considerable potential for use as films or coatings for various food packaging applications.

Incorporation of mineral fillers, especially layered silicate minerals like montmorillonite, into polymers is a strategy to form composite materials with improved mechanical strength and barrier properties. Basically, three different structures may arise, namely *i*) phase-separated composites (microcomposites) wherein the layered minerals are present as stacked particles (tactoids), *ii*) intercalated nanocomposites where polymer chains are intercalated between the silicate layers forming a well-ordered structure, and *iii*) exfoliated nanocomposites where randomly distributed clay layers are dispersed within the polymer in a disordered manner.[6-8] The most widely accepted explanation behind the improved barrier properties is the formation of a more tortuous pathway for permeating molecules, which in turn is related to the diameter of the silicate layers, the extent of delamination of silicate layers and the orientation of individual sheets within the polymer matrix.[7] A number of other factors which may affect the barrier properties of hydrophilic polymers by incorporation of layered silicates have been summarized by Xie *et al*.[9] and include; reduced hydrophilicity compared to unfilled films; shielding of polymer hydroxyl groups by dispersed clay layers; impact on film morphology like free volume, crystal size, degree of crystallinity and presence of macro voids; and formation of strong hydrogen bonds between the polymer and the hydroxyl groups on layered silicates. Even though there are not many easily accessible hydroxyl groups on montmorillonite, such bond formation would act to reduce the diffusion of water molecules through polymer-clay composite films.

Compatibility between polymers and mineral fillers is crucial for the formation of well-dispersed composite structures on the nanoscale and compatibility is gained by matching polarities of the materials.[10,11] Intercalation or exfoliation of the clay particles are favored if the hydrophilicity/hydrophobicity of the polymer and clay are matched.[12] Organophilic modification of clays by exchange of the naturally occurring alkali or alkaline earth metal ions by organic cations can give the clay surfaces a lower surface energy, which may increase their compatibility with a number of hydrophobic polymer matrices.[6,13] These organic modifiers are often cationic alkylammonium or alkylphosphonium surfactants. The presence of bulky alkylammonium ions in the clay interlayer lead to much higher basal spacing, thus enhancing the potential of polymer intercalation.[6,10,11]

Successful intercalation and exfoliation of hydrophilic hectorite and montmorillonite clays in water-soluble PVOH has been reported e.g. by Carrado *et al*.[14] whereas addition of organophilic nanoclays to hydrophilic starch led to the formation of microcomposites.[9,12,15] In contrast, organophilic modified clays have proven to be more effective in promoting intercalated or exfoliated structures in organophilic matrices like polylactide.[16] Natural (unmodified) montmorillonites are easily dispersed in water due to their polar character[11] and are thus compatible with water-soluble polymers like PVOH. The industrially preferred technique to process polymer nanocomposites is the melt intercalation process though solvent mixing and in situ polymerization are also widely adopted methods. Exfoliation in solution has been extensively used for formation of nanocomposites with water-soluble polymers like PVOH.[6]

The presence of polar groups on non-polar polymers in some instances has demonstrated a positive effect on the degree of intercalation with organomodified montmorillonites. Alexandre and Dubois[6] showed that only a low content of polar vinyl acetate groups (from 4.2 mol%) in ethylene-vinyl acetate copolymers was required to favor the formation of intercalation-exfoliation structures whereas with HDPE only intercalated structures were formed. This study contrasts that herein in

that non-polar 'vinyl' groups are present on the polar 'hydroxyl' polymer. The investigation of an organoclay in comparison to that of unmodified clays is therefore justified.

In this study, three different bentonite clays were incorporated at selected concentrations in EPVOH. Composite films were solution cast from aqueous dispersions. One of the major objectives was to study how an organophilic, organomodified clay interacts with the hydrophobically modified polymer. The water vapor permeability and oxygen permeability of the composite films at various RH or after heat treatment were analyzed. Water absorption at different RH's and film dissolution in water were also studied together with thermal properties of the composite films. The distribution of clays was assessed by X-ray diffraction (XRD) and Fourier transform infrared spectroscopy (FTIR).

EXPERIMENTAL

Materials

An EPVOH grade with a degree of hydrolysis (DH) of 97.5-99 mol% and a viscosity of about 25-30 mPas in a 4% water solution at 20°C (determined by a Brookfield synchronized motor rotary type viscometer) was used. The EPVOH is a development product supplied by Kuraray Europe GmbH (Frankfurt a.M., Germany). The product contains <3 wt% methanol and <5 wt% volatiles and was used without further purification. The molecular weight, M_w, was previously determined to be 61,200 g/mol by size exclusion chromatography and the ethylene content was estimated to be about 8.1 mol% by proton NMR analysis[5]. A standard, unmodified PVOH grade with equal viscosity and degree of hydrolysis and with M_w 71, 500 g/mol from the same supplier was used as a reference material.

Three different bentonites were used. Cloisite® Na^+ (here denoted Na-MMT) is an unmodified bentonite from Southern Clay Products Inc (Gonzales, TX, USA) with a cation exchange capacity (CEC) of 92.6 meq/100 g clay. The platelets are 1 nm thick with a diameter of 75-100 nm. PGN® is also an unmodified bentonite, from Nanocor (Arlington Heights, IL, USA) which mostly contains Na^+ exchangeable cations but also a small portion of Ca^{2+} (here denoted C-MMT). More significantly, C-MMT has a larger layer diameter of 300-500 nm and a higher CEC value (120 meq/100 g) compared to Na-MMT. Dellite® 67 G, is an organically modified bentonite from Laviosa Chimica Mineraria (S.p.A., Livorno, Italy) with CEC of 105 meq/100 g clay and aspect ratio of 500. The majority of the naturally occurring sodium ions have been replaced by dimethyl-dihydrogenated tallow ammonium ions, $(CH_3)_2N^+(HT)_2$ and the clay is hence denoted Q-MMT here where Q stands for the quaternary ammonium surfactant. Extensive characterization of the bentonites has confirmed the supplier's claims in that they contain more than 95 wt% montmorillonite.

Methods

EPVOH was dissolved in water to a concentration of 10 wt% by holding at 95°C for 60 minutes under continuous stirring. The clays were used without pre-treatment and polymer-clay composites were formed by addition of 3, 6, 9 or 12 parts dry clay per hundred parts of dry polymer to the polymer-water mixture whilst heating. Further addition of water was used to adjust the final concentration of dry matter to 10 wt% in all mixtures.

Film casting and evaluation of film properties

Films were cast by pouring 10 g polymer-clay dispersions in polystyrene Petri dishes with a diameter of 90 mm, followed by drying at 23°C and 50% relative humidity (RH) for at least five days until further treatment or analysis. By keeping the solids content and mass of dispersion transferred to the Petri dish constant, it was possible to form composite films of almost identical thickness, independently of composition. The minor changes in the film density due to the low addition levels of fillers were assumed to have negligible effect on the film properties.

The final film thickness was recorded by a thickness tester (Lorentzen & Wettre type 532 G, Stockholm, Sweden) on at least five locations of each film. The casting method resulted in a film thickness of around 100 µm. In a previous study it was demonstrated that the barrier properties of EPVOH films reached a plateau value with a film thickness of ca. 50 µm[5], it can therefore be assumed that minor variations in film thickness have a negligible impact on the barrier properties.

Heat treatment is generally utilized to enhance the water resistance of PVOH films since the degree of crystallinity increases almost linearly with the applied temperature during heat treatment.[17] An annealing temperature of 120°C for 10 minutes was selected for EPVOH-clay films because it did not induce any discoloring (yellowing) indicative of degradation.

Water vapor transmission rate

The water vapor transmission rate (WVTR) was measured by the gravimetric cup method (ASTM E96) using silica gel as desiccant. Aluminum cups fitted with sample holders (lids) giving an exposed film area of 50 cm^2 were used. The cups were firmly tightened by placing a rubber O-ring on one side of the film whereas silicon grease was used to prevent leakage between the film and the aluminum ring on the other side. The cups were placed in a climate chamber (C+10/200, CTS Clima Temperatur Systeme GmbH, Hechingen, Germany) and pre-conditioned for 24 h prior to analysis of WVTR in an atmosphere of 23°C and 80% RH.

Oxygen transmission rate

The oxygen transmission rate (OTR) was measured according to ASTM D3985-05 by a Mocon® OxTran® oxygen transmission rate tester, Model 2/21 (Mocon Inc., Minneapolis, MA, USA), equipped with a coulometric oxygen sensor. An adhesive aluminum foil mask was used to envelop the films, leaving an exposed test area of 5 cm^2. The oxygen concentration in the test gas was 21% and the carrier gas was a blend of 98% nitrogen and 2% hydrogen. Measurements were carried out in duplicates at 23°C and 80% RH under atmospheric pressure. Pre-conditioning in the test chambers was done for 10 h and measurements were run until steady state was reached.

Moisture content and dissolution in water

The equilibrium moisture content of all films stored at 23°C in an environment of either 50% RH or 80% RH for at least 24 h were recorded by weighing small pieces cut from each film, followed by drying at 105°C for >1 h (until constant weight; assuming complete removal of water) and subsequent re-weighing. Measurements were performed in triplicates. The moisture content was calculated by Equation (1):

$$Moisture\ content = \frac{W_0 - W_d}{W_0} x\ 100 \quad (1)$$

where W_0 is the initial weight of the film and W_d is the weight after drying.

The moisture content of the fillers were recorded by storing small portions of each powdered clay for 24 h at 23°C and at two relative humidities: 50% RH and 80% RH, followed by weighing and drying as above until a constant weight was achieved. The dissolution of films in water is described in the Supplementary data.

XRD

X-ray diffraction traces of clay powders and composite films were obtained using a Philips X'Pert Pro diffraction system using a Cu-tube (λ = 1.542 Å), operating at 40 kV and 40 mA.

FTIR

FTIR spectra were collected using a Specac, single pass, attenuated total reflectance Golden Gate™ accessory on a Nicolet, Nexus spectrometer.

Thermal properties

A modulated differential scanning calorimeter, Q2000 (TA Instruments, New Castle, DE, USA) was used for studying the thermal properties of polymer films. Film pieces of ~10 mg were placed in Tzero aluminum pans and hermetically sealed. Pure PVOH and EPVOH film pieces were investigated from three replicates of *i*) films dried at 23°C and 50% RH; *ii*) films with high moisture content (conditioned at 80% RH) and *iii*) essentially water-free films (oven dried at 105 °C for 90 min). All composite films were analyzed after drying at 23°C and 50% RH and those containing 6 pph clay also after annealing at 120°C. The thermal properties of the clays were investigated using powders dried at 105°C for 24 h. All samples were heated from -20°C to 250 °C using an oscillating heating rate of 0.32°C/min overlaid on a linear heating rate of 2°C/min. The modulated technique allows heat flow due to heat capacity changes, e.g. glass transitions (reversing heat flow) to be separated from heat flow changes due to kinetic events such as melting, volatilization and decomposition (i.e. non-reversing heat flow). Glass transition temperatures, T_g, were taken from the inflection point on the reversing heat flow curve whereas melting temperatures and enthalpies were recorded from the non-reversing heat flow curves.

RESULTS AND DISCUSSION

Film properties

The cast composite films were visually homogeneous, with smooth surfaces and contained no visible particle agglomerates. Incorporation of clays promoted the formation of planar films with no tendency to curl or to separate from the Petri dish at the center of the film. This contrasts with the occasional behavior of the unfilled EPVOH film in which uneven drying processes caused faster drying regions of the film to separate from the Petri dish whilst the wet regions remained flat. The presence of the dispersed clay particles introduces physical cross-links into the film structure which act to conserve the dimensional stability of the film. Consequently, the size change upon drying is less pronounced.

Whereas the pure EPVOH films, EPVOH/C-MMT and EPVOH/Na-MMT composite films remained planar upon additional drying at 105°C, the EPVOH/Q-MMT films curled from the edges towards the center and more so with higher loadings. Partial settling of the Q-MMT particles during initial film preparation, as evidenced by XRD and FTIR and discussed below, may have caused uneven tension in the thickness direction of the films and thus variations in drying rates in the upper and lower portions of the film leading to curling.

The XRD trace for a cast EPVOH film was featureless and rose slightly towards lower angles (Figure 1). The peak observed at 19.1 °2θ represents the semi-crystalline nature of the EPVOH, which is analogous to that of PVOH[18] and acts as an internal reference to the height of the clay diffraction peaks.

The peak at 6.9 °2θ in the traces of the Na-MMT and C-MMT powders is associated with a d_{001} spacing of 12.8 Å. The absence of this peak in the traces obtained from Na-MMT and C-MMT composite films combined with the increasing baseline at angles <5 °2θ indicates[19] that the clay in these samples is very well dispersed and disordered, if not exfoliated (Figure 1 a, b). The extent of the increasing baseline correlates with the filler loading and is associated with an increasing amount of X-ray scatter due to the nanoscale dispersion of the clay layers. Breen *et al*.[20] also reported the absence of diffraction peaks in PVOH-Cloisite Na^+ nanocomposite films at clay additions below 25 wt%, which was taken as a confirmation of extensively dispersed clay platelets in the polymer matrix. Furthermore, Khairuddin[21] studied adsorption isotherms of PVOH with M_w ~30,000 g/mol on the same clay and XRD analysis indicated the presence of both predominantly intercalated structures with > 25 wt% clay and predominantly exfoliated structures with <10 wt% clay. They showed that the d-spacing increased from about 12 Å for untreated clay to about 40 Å at 75 wt% PVOH. The results indicated that PVOH was present in clay galleries as a fully formed bi-layer at 25 wt% PVOH and that the amount of PVOH in the interlayer significantly and gradually increased as the amount of PVOH offered rose from 25 to 75 wt%.

It was not possible to unequivocally determine whether the EPVOH was present in the interlayer of Q-MMT. Vaia[19] advised caution when seeking to attribute small increases in basal spacing to the presence of extra material in the interlayer so the slight shift to lower angles of the d_{001}-spacing from the Q-MMT powder to that in the composite films (2.5 to 2.23 °2θ, respectively) will be disregarded. However, it is very clear that the d_{002} (3.9 °2θ) and d_{003} (6.9 °2θ) peaks become more prominent and resolved, thus demonstrating improved ordering of the clay layers either in stacks or by the arrangement of stacks in the film. This change could be due to re-arrangement/re-distribution of the organomodifier, and/or removal of excess modifier from within the interlayer region; all resulting from the extra processing that occurs during the preparation and casting of the EPVOH composite films.

Generally, the intensities and shapes of the diffraction peaks were similar from a number of traces collected from the same side of a film sample for all EPVOH-clay composites suggesting a homogeneous distribution at both the top and bottom surfaces. However, for the Q-MMT samples there was no clear correlation between the peak intensity and loading (Figure 1 c, d). For example, the trace collected from the top surface of the 3 pph Q-MMT composite indicated a low amount of clay present, whereas that from the bottom surface suggested a higher amount of clay. The differences in peak intensities collected from top and bottom surfaces do indicate settling, i.e. the

presence of a graded film structure with a low fraction of Q-MMT at the top surface and a high fraction at the bottom.

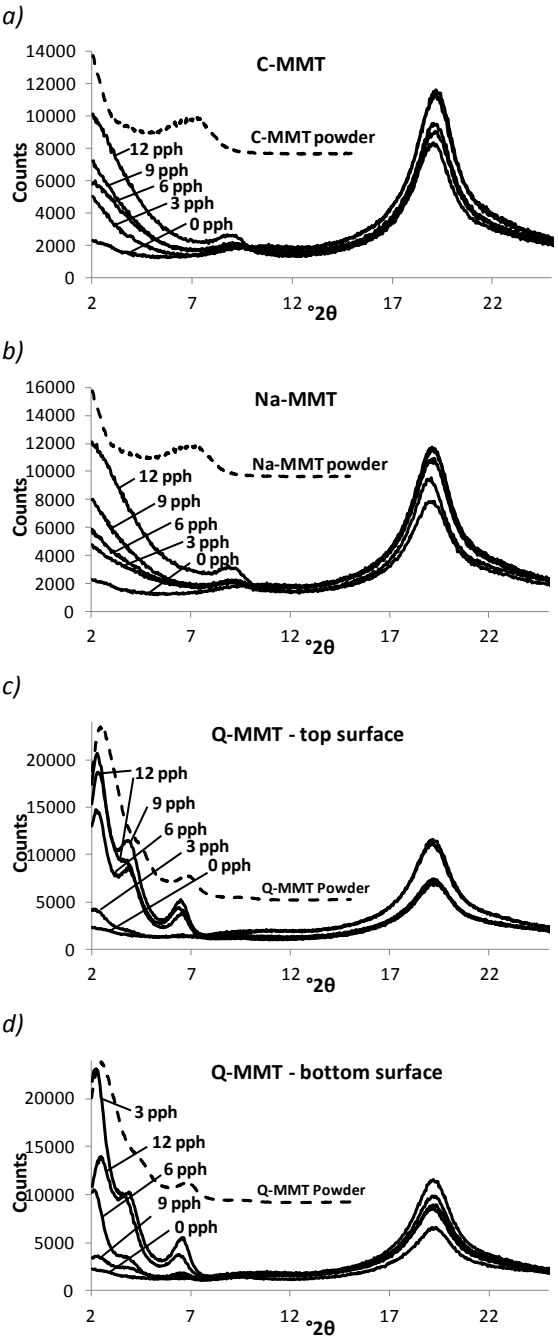

Figure 1. Typical XRD patterns of a) C-MMT, b) Na-MMT composite films. In c) and d) the XRD patterns of the Q-MMT composite films recorded from the top and bottom surfaces respectively are shown. Dashed lines show the patterns collected from the clay powders and are offset for clarity.

FTIR spectra were recorded from both the top and bottom film surfaces to further investigate the film homogeneity. The depth of penetration of the infrared beam is ~2-12 µm, which means only the film in contact with the ATR prism contributes to the FTIR spectrum (total film thickness ~100µm). For all samples, the spectra collected from each surface at several locations (>6) showed high reproducibility. The pure EPVOH film exhibited a characteristic band at 1085 cm^{-1} representing the C-O stretching in the vinyl alcohol units[22] whereas bands associated with clay were identified at ~1030

and 1045 cm^{-1} (attributed to the Si-O stretching usually reported in the range 1150-950 cm^{-1} for montmorillonite)[20,23]; Figure 2. The intensities of the clay bands increased with increasing amounts of C-MMT or Na-MMT and were of similar intensity for both the top and the bottom surfaces, thus suggesting that similar amounts of these clays were present at both surfaces. However, no clay was evident in the top surfaces of the Q-MMT composites since the spectra were almost identical to that of the pure EPVOH film. In contrast, bands at ~1030 cm^{-1}, which were identified in the spectra recorded from the bottom surface, increased in intensity with increased clay loading. Furthermore, comparison of the relative intensities of the bands at ~1030 cm^{-1} with those at 1085 cm^{-1}, demonstrated that higher amounts of clay were present at the bottom surfaces of the Q-MMT composite films than the corresponding samples containing Na-MMT or C-MMT. The FTIR data thus strongly suggests that Q-MMT partially sediments during the drying stage because of the weak interaction with EPVOH. This weak interaction between Q-MMT and the polymer was also observed by rheology assessments in the wet state.[5]

a)

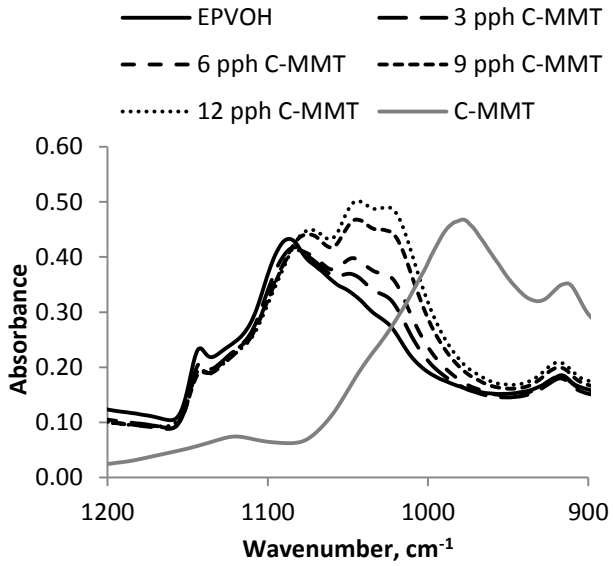

b)

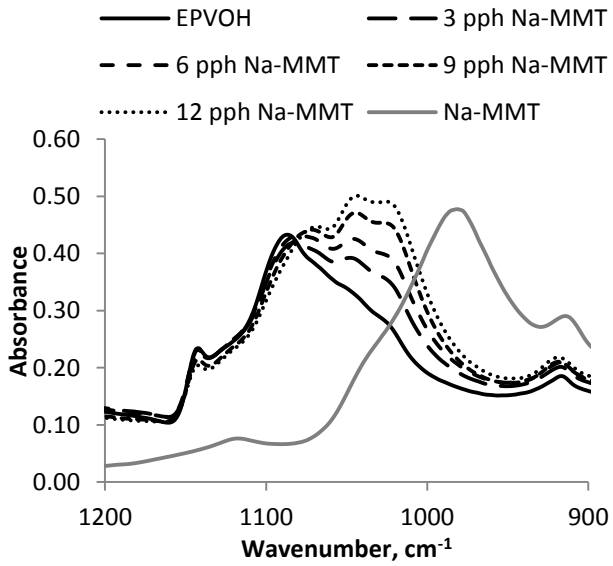

c)

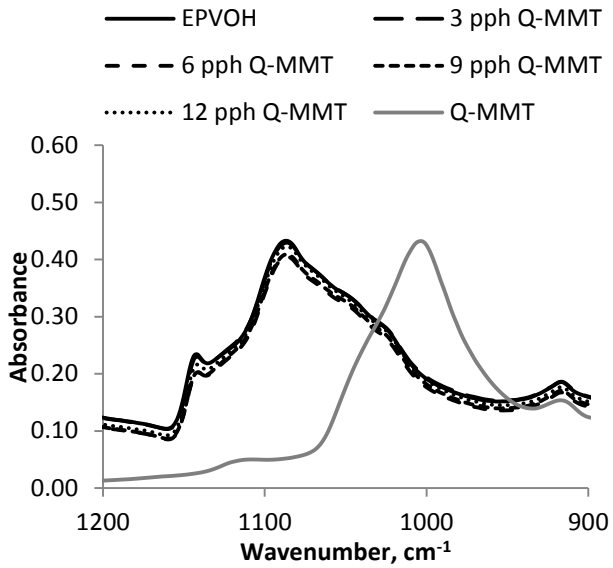

d)

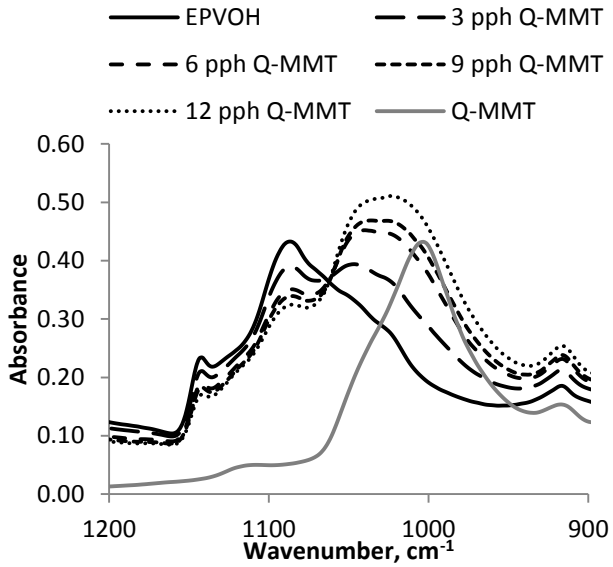

Figure 2. FTIR spectra of a) C-MMT, b) Na-MMT composite films. In c) and d) the spectra of the Q-MMT composite films recorded from the top and bottom surfaces respectively are shown.

Water vapor permeability

Figure 3 presents the water vapor barrier properties of EPVOH composites measured at 23 °C and 80% RH as water vapor permeability (WVP), in g/Pa·s·m, which accounts for the actual film thickness (100 ± 6 μm for all films), the saturation vapor pressure at the actual test temperature and the RH gradient across the test films, assuming 0% RH inside the cups. For the EPVOH/Q-MMT composite, a 4-fold decrease compared to the unfilled film was achieved by addition of 3 pph Q-MMT. In the case of 3 pph Na-MMT a significant, but lower reduction in WVP was observed, but for 3 pph C-MMT only a marginal improvement was found. Further addition of any of the clays beyond 3 pph caused the WVP to increase and reach a maximum (at 6 pph for Na-MMT and C-MMT and 9 pph for Q-MMT), after the observed maximum the WVP decreased upon further clay addition.

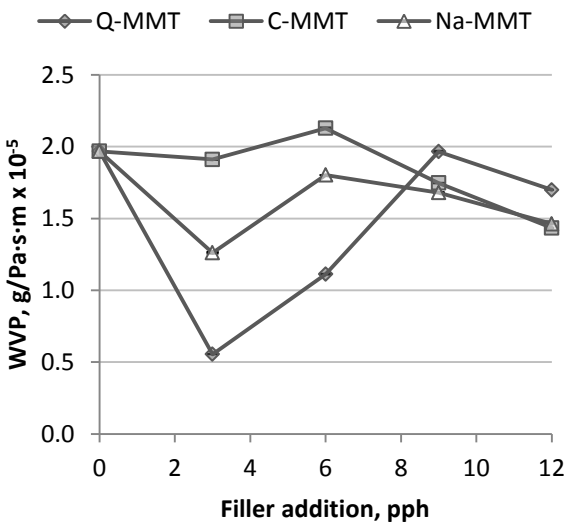

Figure 3. WVP of EPVOH as a function of filler addition at 80% RH. Error bars showing standard deviations are included, but smaller than the data markers. The maximum standard deviation was $0.007 \cdot 10^{-5}$ g/Pa·s·m.

The WVPs of the composite films are closely related to how the clay is dispersed within. At very low loadings of clay (i.e. 3 pph) the dispersion is likely to be optimized due to a lower probability of physical, direct clay-clay interactions. This presumably leads to the enhanced WVP improvement for Na-MMT and Q-MMT composites at this clay content. At higher clay loadings (>6 pph) the extent of dispersion will be less due to there being insufficient volume within the polymer matrix for the clays to exfoliate; the resulting agglomeration of the clay particles may present channels for water to pass through more readily. Above a certain clay concentration, i.e. the observed maximum, the layers are combined such that a closely packed distribution is formed that limits the passage of water vapor.

The combination of Q-MMT and EPVOH resulted in the lowest overall water vapor permeability (<1.0 g/Pa·s·m x 10^{-5}) at the lowest addition of clay, which supports the creation of a highly impermeable and segregated or self-stratifying clay layer within the film, as indicated by the XRD and FTIR data. Perhaps the organophilic Q-MMT clay also contributes to reduce the water sensitivity of the polymer.

Moisture content at equilibrium and moisture uptake at different relative humidity

The equilibrium moisture content (Equation (1)) of PVOH and EPVOH films stored at 23°C and 50% RH was about 9.6% and 8.2%, respectively. After exposing the films at 23°C and 80% RH these values rose to about 15.0 ± 0.4% and 14.8 ± 0.1%, respectively (average from triplicates). Thomas and Stuart[24] showed that equilibrium moisture uptake of PVOH films was reached within <12 hours. Supplementary data shows that both film types absorb increasing amounts of moisture as the humidity is increased incrementally from 50% RH, but the increase is slightly higher for PVOH, especially at RH ≥80%. After annealing the PVOH and EPVOH films at 120 °C for 10 minutes, followed by re-conditioning at 23°C and 50% RH for 24 h, the average moisture content was about 7% and 6.8%, respectively indicating that annealing for 10 min causes a 'permanent' reduction of the equilibrium moisture content of the films.

Hodge *et al*.[25] investigated the water absorption of PVOH films and expressed three states in which water can be present; i) non-freezing water, i.e. that directly H-bonded to the –OH of PVOH, ii) freezable water, i.e. that H-bonded to the non-freezing water, and iii) free water, i.e. that not perturbed by the H-bonding water associated with PVOH. At the initial stages of water absorption, non-freezing water disrupts inter- and intramolecular hydrogen bonding within PVOH. While assuming that one non-freezing water molecule attaches to every –OH group on PVOH (i.e. one H_2O molecule per monomer unit), they concluded that site saturation should be reached at 29 wt% water. Thomas and Stuart[24] also supported the theory of a maximum absorption of non-freezing water of 29%. Calculations show that the replacement of –OH groups by 8.1 mol% ethylene units reduces the amount of water required to reach site saturation in EPVOH to 26-27% (Supplementary data). The data herein suggests that the amounts of water present in the films are considerably below the level of 22 wt% where freezing water is expected.[25]

The clays are, in addition to the polymers, capable of absorbing moisture from the environment. When changing from 50 to 80% RH the moisture content in the organomodified clay only increased from about 2 to about 3% whereas for both C-MMT and Na-MMT, the moisture content was more than doubled (from about 7 to over 15%).

Comparing the equilibrium moisture content in the EPVOH films with those in the hydrophilic C-MMT and Na-MMT clay powders shows that the films contain more bound water at 50% RH (~8.2% relative to ~7%), but contain similar amounts at 80% RH (~15% relative to 15-16%). The presence of clay can influence the size and number of crystallites; the ratio of crystalline to amorphous phases; the free volume; and the connectivity in and between amorphous regions – all of these will influence the amount of sorbed moisture. The specific location of water adsorbed onto clay or EPVOH in composites is difficult to define since when combined, molecular bonding interactions between EPVOH and clay will compete with those between EPVOH or clay with water. This competition, which is dependent on clay/polymer concentrations, will therefore influence the water solubility, the free volume, the amount of water present and also how strongly it will interact.

The moisture content of the EPVOH/Q-MMT composite films at 80% RH decreased linearly (r^2=0.99) with increased clay concentration from 14.8 with no Q-MMT to 13.2% at 12 pph Q-MMT (Figure 4). For EPVOH/C-MMT and EPVOH/Na-MMT a slight reduction in moisture content with increased clay load was also observed even though the trends were not as clear as with Q-MMT. The presence of clay will affect polymer folding and larger amounts of clay are supposed to give less crystalline films, but it is not clear whether the observations are related to free volume effects. However, it can be asserted that the presence of hydrophilic clays did not lead to increased absorption of moisture in the films when exposed at high relative humidity.

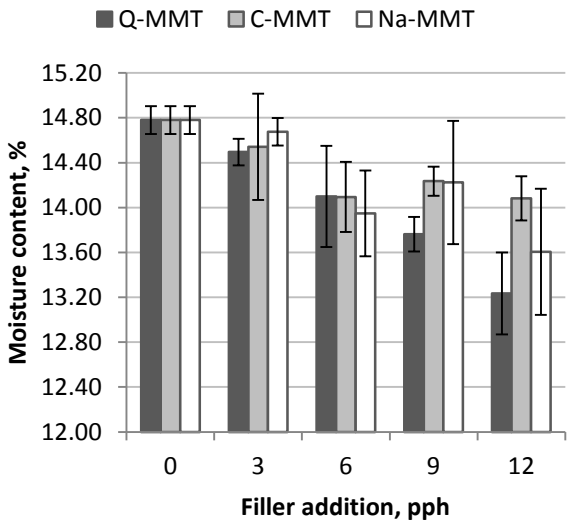

Figure 4. Moisture content in composite films as a function of filler content calculated by Equation (1). Films exposed at 80% RH for 24 h. Average of three measurements. Error bars represents standard deviation.

Oxygen permeability

Figure 5 shows the oxygen permeability (OP) measured at 23 °C and 80% RH as an effect of filler addition. The values are expressed in $cm^3 \cdot cm/m^2 \cdot d \cdot bar$ thus taking into account the actual film thickness. Comparative data for OP values of conventional packaging films showed that the OP of unfilled EPVOH at 80% RH was more than two orders of magnitude lower than for LDPE, almost five times lower than for PVOH and almost identical to the value for PET.[5]

Increasing amounts of C-MMT or Na-MMT in EPVOH resulted in similar linear (r^2>0.98) decreases as OP reduced from about 2.5 to 1.0 $cm^3 \cdot cm/m^2 \cdot d \cdot bar$ when going from 0 to 12 pph filler. As with the WVP results (Figure 3) Q-MMT showed an optimum OP performance at 3 pph. Although OP slightly increased with addition of 6 and 9 pph it was still an improvement over the film with no clay. When compared with the other two clays at corresponding addition levels the incorporation of organophilic clay was effective only at very low addition levels. Despite considerable scattering in data, there is a downward trend in moisture content with increased concentration of C-MMT and Na-MMT (Figure 4). This reduction in moisture, along with the physical barrier properties that the clay constitutes may explain the improvement in OP with C-MMT and Na-MMT. With Q-MMT the moisture content substantially decreased with increasing clay content and thus a respective decrease in OP may be expected; however it was found to act best as a barrier to oxygen at low loadings (3 pph). A distinctly different type of dispersion of Q-MMT (as shown by XRD and FTIR), compared with Na-MMT and C-MMT, due to the limited chemical compatibility between the highly organophilic particles and the less hydrophobic polymer matrix may promote channels for oxygen to proceed through the polymer matrix at higher addition levels.

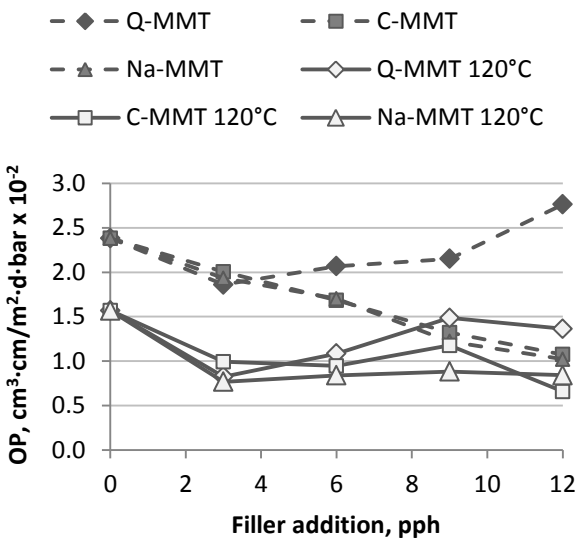

Figure 5. OP of EPVOH films as a function of filler addition (filled symbols), and of annealed films (120°C) (open symbols). Average of two measurements at 23°C and 80% RH with maximum standard deviation of 0.43 (non-annealed) and 0.33 (annealed) ·10^{-2} cm^3·cm/m^2·d·bar.

Figure 5 also shows that annealing the EPVOH film at 120°C for 10 minutes led to a reduction in OP by a factor of 1.5. Annealed composite films containing 3 pph of any filler resulted in OP values at or below 1.0 cm^3·cm/m^2·d·bar equating to a reduced OP by a factor of 2.1-2.5 when compared to the non-annealed films. For annealed films containing C-MMT and Na-MMT, no further reduction in OP was observed with increased filler addition, whereas the Q-MMT films expressed a minimum at 3 pph. The OP for Q-MMT films then increased with further filler addition, as observed for the non-annealed films. Here it could be concluded that incorporation of 3 pph of Na-MMT caused a reduction of OP by a factor 1.2 whereas the combined effect of 3 pph Na-MMT and annealing led to a reduction in OP by a factor of 2.0. Similar summative effects were also achieved with the other two clays, at least at the lowest addition level.

An effect of the annealing process is that the moisture content in the films is reduced, which is one possible mechanism for the observed reduction in OP values. Another possible effect is a change in film crystallinity. This aspect, in combination with effects on dissolution in water, is further discussed in Supplementary data.

Comparison between experimental data and permeability models

The models based on the formation of a tortuous path for reduction in permeability of polymer composites (P_c) to the permeability of the pure polymer (P_p) proposed by Nielsen in the 1960s and later revised by Cussler and co-workers in the 1980s have proven to be good predictions of P_c/P_p for films with volume fraction of fillers below 10%.[26]

Even though most particle movement will take place in the hydrated pre-film, the comparatively large thickness (~100 µm) of the films in this study should allow the platy clay particles to rotate freely and adopt a random distribution in the films, at least at the lowest concentrations of clay and the lowest aspect ratios of the clay layers. Bharadwaj pointed out that for clay particles with large aspect ratio (length > 500 nm), the dependence on the relative orientation of the particles is reduced

and a random orientation might be as effective for the barrier properties as alignment perpendicular to the diffusing path, which may ultimately override a lack of complete delamination.[7] A comparison between experimental OP data and values of P_c/P_p predicted by the model proposed by Bharadwaj[7] was undertaken using Equation (2):

$$\frac{P_c}{P_p} = \frac{1-\phi_f}{1+\frac{L}{2W}\phi_f\left(\frac{2}{3}\right)\left(S+\frac{1}{2}\right)} \quad (2)$$

where ϕ_f is the volume fraction of fillers, while *L* and *W* are the length and width of silicate sheets. *S* is an order parameter which is equal to zero in case of random orientation of the sheets. When *S* = 1, which corresponds to planar arrangement of sheets (perpendicular to the film surface), Equation (2) is reduced to the equation originally proposed by Nielsen. Figure 6 shows the ratio of oxygen permeability of the Na-MMT and C-MMT composite films to the pure EPVOH film plotted against the volume fraction of fillers, ϕ_f. Since the specific gravity of C-MMT (2.60 g/cm^3) is slightly lower than for Na-MMT (2.86 g/cm^3), addition of an equal weight fraction of clay implies that C-MMT will occupy a higher volume in the composite, which is illustrated by the marginal shift of ϕ_f to higher values. Also shown are the corresponding relative permeabilities calculated by Equation (2) for the example cases of *L* set to 100 (Na-MMT) and *L* set to 500 (C-MMT) respectively, with the order parameter settings *S* = 0 and *S* = 1. The sheet width *W* was set to 1 nm. For EPVOH/Na-MMT a perfect match between experimental data and the Bharadwaj model for *S* = 0 was found, which suggest a completely random orientation of the silicate sheets in the film. The higher aspect ratio of C-MMT results in predicted permeability values that are much lower than for Na-MMT. However, experimental data for EPVOH/C-MMT composite films lie close to those for EPVOH/Na-MMT. The model thus indicates that C-MMT is not fully delaminated into homogeneously dispersed layers, which is in contrast to the XRD data which suggested that C-MMT particles are highly disordered, probably exfoliated (Figure 1).

Nazarenko *et al*.[26] concluded that for polystyrene/MMT composites, the oxygen permeability was strictly dependent on the diffusivity, i.e. a pure tortuosity effect, and that the effect of the mineral phase on the solubility was negligible at $\phi_f < 0.1$. However, a smaller reduction in permeability than anticipated by the Nielsen and Cussler models was observed, which was attributed to layer aggregation. They modified the Nielsen model to take into account the presence of homogeneously dispersed, randomly oriented layer stacks (aggregates) with the number *N* of layers per stack (varying between 3-9). Adopting a similar calculation for the EPVOH/C-MMT composite by using *L* = 500 nm, and selecting *N* = 6 allowed a prediction of P_c/P_p that lay very close to the experimental data (Figure 6). An explanation of the mismatch between XRD data and the model fitting could be that C-MMT is present as stacked layers with a highly random orientation or that smearing of the clay layers has occurred. The effect of these processes would not be observable in the x-ray diffraction patterns.

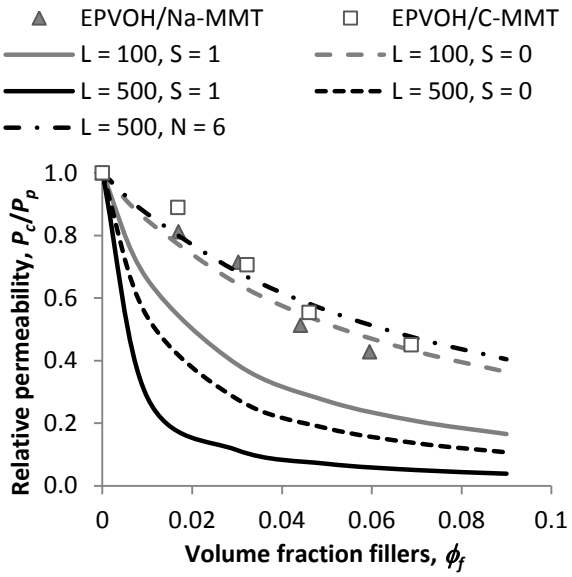

Figure 6. Relative oxygen permeability of EPVOH/Na-MMT and EPVOH/C-MMT composite films with fittings to various models.

Performing a similar model fitting for EPVOH/Q-MMT suggested the presence of stacks with N = 9, 30 and 90 layers for 3, 6 and 9 pph Q-MMT respectively, hence the aggregate size increased with increased addition of clay. These considerably higher values of N will also reflect that the clay is within concentrated boundaries; recall that the XRD and FTIR data (Figures 1 and 2) show they are not dispersed evenly throughout the film. At 12 pph Q-MMT, the OP was higher for the composite than the pure polymer, which is considered to indicate the occurrence of voids in the polymer matrix due to the presence of large aggregates. It should be noted that due to the considerably lower specific gravity of Q-MMT (1.70 g/cm^3) compared to the values for Na-MMT and C-MMT, the volume occupied by the 3 pph Q-MMT added is as large as for addition of 6 pph Na-MMT or C-MMT (ϕ_f ~ 0.03) and further so with increased weight loads.

Thermal properties

Thermal properties of polymers

The EPVOH film dried at 105°C for 90 min showed an average T_g of 71.8°C (Figure 7a - labeled Dry), whereas the corresponding value for PVOH was 70.5°C. These figures are close to the 72.1°C reported elsewhere for pure PVOH[27] and to the T_g of 72°C for EVOH films with ethylene content of 27 mol%.[2]

Within crystalline domains no water molecules are present, whereas in the amorphous regions pockets of water might exist. Hodge *et al.*[25] showed by DSC that for a water content in the amorphous region of PVOH films below 22 wt%, all water is associated with the polymer as non-freezing water, i.e. hydrogen-bonded water not possessing sufficient structural order to undergo detectable bulk water phase transitions. Water is an effective plasticizer for PVOH[17], especially in the form of non-freezing water.[28] This plasticizing effect is illustrated in Figure 7a by a reduction in T_g for EPVOH to 22.9°C when stored at 50% RH (moisture content 8.2%) and to -3.8°C when equilibrated at 80% RH (moisture content 14.8%). The corresponding values for PVOH were 23.8°C and -5.4°C, respectively. Both polymers showed a perfectly linear decrease in T_g from the dry state with

increasing moisture content (r^2=0.99). The trend in results are in line with Hodge *et al*.[28] who reported a single glass transition temperature by DMA for each water content of PVOH films with T_g of 30°C at 8 wt% water and T_g of 22°C at 10 wt% water. As mentioned above the recorded moisture contents at 80% RH in the present study are well below the critical 22 wt% level for water to freeze and since MDSC provided no evidence to suggest otherwise, it is assumed that no freezable or free water was present in the samples during these investigations.

a)

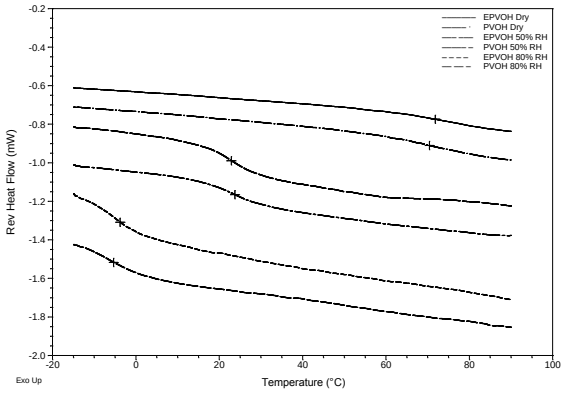

b)

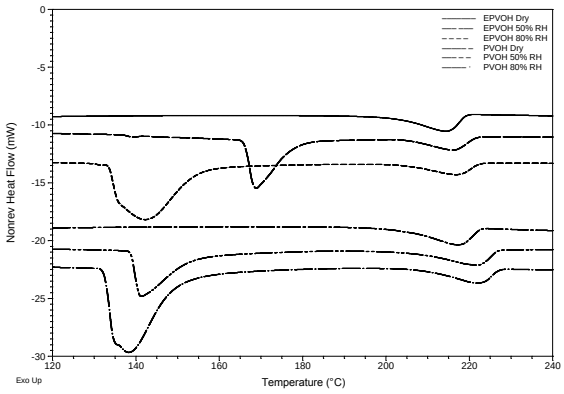

c)

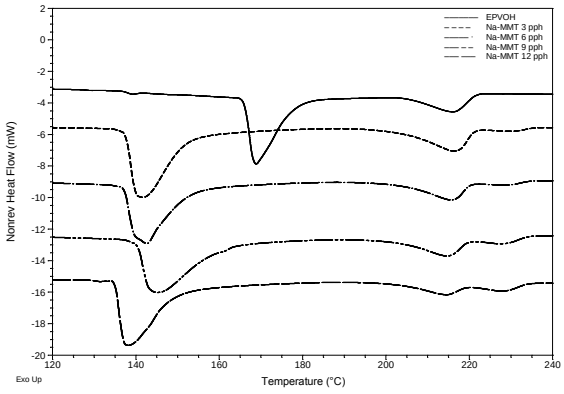

Figure 7. DSC curves for EPVOH and PVOH dry films and films exposed to 50% and 80% RH. a) reversing heat flow curves, glass transitions are marked with a cross, b) non-reversing heat flow curves showing endothermic transitions. c) non-reversing heat flow curves for EPVOH/Na-MMT composite films conditioned at 23°C and 50% RH.

Storage and testing of the films at 23°C means that the surrounding temperature is at or close to the T_g of the film when at 50% RH or significantly higher than the T_g of the film at 80% RH. This means that the EPVOH polymer is in the rubbery state in the latter case, i.e. the molecules will have substantially higher mobility thus possibly leading to the formation of a more amorphous structure. It is therefore also more likely that the ingress of water into the polymer will create a path for both water and oxygen molecules to diffuse through the matrix, thus leading to the observed increase in permeability of water vapor and oxygen with increased RH.[5]

The non-reversing heat flow curves presented in Figure 7b of the dry EPVOH film showed a melting endothermic event at 214°C with an average melting enthalpy (ΔH_m) of 50 J/g. The corresponding values for dry PVOH were 217°C and 45 J/g, respectively. These figures are comparable to data for PVOH reported elsewhere. For example, Tubbs and Wu[29] reported crystalline melting points in the range 212-235°C for isotactic PVOH whereas Mallapragada and Peppas[30] observed melting points in the range 190-235°C depending on the molecular weight of PVOH; Strawhecker and Manias[31] further identified a bulk T_m of 225°C for a fully hydrolyzed atactic PVOH.

The average values of T_m and ΔH_m for PVOH were 222.1°C and 38.0 J/g (at 50% RH) and 222.4°C and 38.4 J/g (at 80% RH), i.e. a shift to slightly higher melting temperature and lower melting enthalpy compared to the dry film was found, the data was independent of the moisture level. For EPVOH the corresponding values were 215.3°C and 36.0 J/g (at 50% RH) and 217.6°C and 37.4 J/g (at 80% RH), again the magnitude of the enthalpy changes did not correlate with the moisture content of the films. Annealing the EPVOH film at 120°C for 10 minutes resulted in a melting enthalpy of 42 J/g which indicates a slightly higher degree of crystallinity compared to the films stored at 23°C and 50% or 80% RH but, as anticipated, a lower crystallinity than in the dry film (ΔH_m ~ 50 J/g).

Strong endothermic transitions were observed between the T_g and T_m events in the non-reversing heat flow curves for both EPVOH and PVOH films when dried at 23°C and conditioned at 50 or 80% RH. Hermetically sealed Tzero pans were used in the MDSC trials and these are designed to suppress volatilization of adsorbed water (in for example polymeric films), a process which normally becomes visible as a broad endotherm centered around 100°C in the non-reversing heat flow curve. Nevertheless, it is believed that the endothermic events observed are due to evaporation of water since these peaks were absent in the MDSC traces for the dry polymer films (Figure 7b). For EPVOH, this transition occurred at an average temperature of 167°C with an average enthalpy of 94.5 J/g when dried at 50% RH (Figure 7b) whereas for PVOH the corresponding endothermic transition occurred at a much lower temperature (142°C) with an enthalpy of 60.2 J/g. After exposure of the films to 80% RH, there was a shift of this endotherm to lower temperature (around 143°C for EPVOH and around 137°C for PVOH) and a simultaneous broadening of the peaks (Figure 7b). The high temperatures at which these endothermic transitions take place indicates that water is very strongly associated with the polymers. The observations are analogous with Breen *et al*.[20] who found by TG-MS analysis that the temperature over which water was evolved from a pure PVOH film reached a maximum at 140°C. The authors also observed that the peaks became broader and that T_{max} shifted to lower temperature with increased content of water, i.e. reminiscent of the peaks depicted in Figure 7b.

The enthalpy of the endothermic transitions in the range 140-170°C increased by a factor of 2-4 (from 94.5 to 233.6 J/g for EPVOH and from 60.2 to 235.2 for PVOH) when comparing films exposed

to 80% RH with those exposed to 50% RH, which confirms a strong coupling between this transition and the water content in the films. In addition, the DSC curves shows two overlapping endothermic transitions near 140°C for both PVOH and EPVOH exposed to 80% RH (Figure 7b). This indicates that water is present in at least two different environments within the films, one where the water is more strongly bound to the polymer than the other.

Thermal properties of composites

The glass transition temperature increased step-wise from 22.9°C for the pure EPVOH film to 25.5°C with the highest addition level of Q-MMT (12 pph). An increase in T_g has been ascribed to restricted segmental motions due to the presence of the clay[6] since segmental motion is impeded whenever a polymer comes in contact with a surface. From the MDSC experiments there was no evidence to support that the organomodifier promoted plasticization since the T_g was not reduced, which was observed, for example with organomodified clay (Cloisite® 30B) in poly(acrylated oleic methyl ester).[32] For the Na-MMT and C-MMT composite films, T_g remained similar to that of unfilled EPVOH, which is anticipated since with very well dispersed and highly disordered (or exfoliated) systems fewer restrictive environments will be present to affect segmental mobility.

The T_g after annealing the EPVOH films at 120°C and re-conditioning at 23°C and 50% RH for 24 h was 24.5°C (moisture content 6.8%), which was an increase of 1.6 °C compared to the corresponding non-annealed film (8.2% moisture). The composite films containing 6 pph of any of the three fillers (and with less moisture content, 4.9-6.3%) all showed similar T_g values between 24.1-25.6°C after annealing and an average upward temperature shift of 1.6-2.4°C.

The weak melting transition (T_m) found in pure EPVOH at about 215°C (at 50% RH) was essentially unaffected by the presence of C-MMT or Na-MMT (exemplified by Na-MMT composite films in Figure 7c) whereas the transition took place at a slightly higher temperature (217°C) for all the Q-MMT films. The melting enthalpy of this transition decreased gradually with increased filler content for all clay grades. For Na-MMT (Figure 7c) a linear decrease (r^2=0.98) from 38.0 J/g to 12.5 J/g was observed when going from 3 to 12 pph Na-MMT, which is significantly greater than the minor reduction in the polymer concentration by addition of clay and so reflects a decreased degree of crystallinity of the bulk polymer phase.

The composite films showed the same strong endothermic transitions between T_g and T_m as the pure EPVOH. For Q-MMT composites, an upward shift from 167 °C for pure EPVOH to 169-181°C was observed, with a weak trend towards increased temperature with increased amount of clay while the enthalpy moved in the opposite direction (decreasing from 83 to 72 J/g from 3 to 12 pph Q-MMT). For C-MMT the peak temperature decreased from 162°C (3 pph) to 141°C (12 pph) with an accompanying increase in enthalpy from 95 to 117 J/g. With Na-MMT the transition was located around 140°C, whereas the enthalpy decreased from 127 to 122 J/g from 3 to 12 pph Na-MMT.

After annealing there was a downward shift of the first endothermic peak to about 146°C for EPVOH and to 148°C for the 6 pph EPVOH/Q-MMT composite film, with minor changes in enthalpy. In contrast, the temperature at which the transition occurred was unaffected by annealing (within error limits) in the 6 pph C-MMT and Na-MMT composite films. For the latter films, there was however a marked enthalpy reduction from 113 to 79 J/g (C-MMT) and from 124 to 92 J/g (Na-MMT).

The transitions observed in the pure clay minerals (not shown) did not contribute to the traces recorded for the composite films. In addition, the results show that the polymer phase dominates the thermal properties of the composite films and that the fillers did not have any major effect on the overall properties at the different filler levels utilized. Moreover, it could be concluded that the moisture content had a greater impact on the glass transition temperature than did the filler concentration.

The endothermic reaction in the mid-range region took place at higher temperatures in the EPVOH and EPVOH/Q-MMT composite films when compared to the Na-MMT and C-MMT composites. In addition, for both C-MMT and Na-MMT the transition enthalpies increased with filler addition. This difference in thermal behavior raised a question as to whether this transition was solely related to evaporation of water or if it could also be connected with the presence of different types of crystallinity (e.g. crystallite size or form) in the different films. Strawhecker and Manias[33] reported the appearance of a new crystalline form of PVOH with a T_m higher than that of the bulk crystalline form (i.e. >225°C) upon addition of MMT fillers. They observed that the enthalpy of this latter melting transition increased with increased fraction of fillers at the expense of the enthalpy of the bulk-like crystals. In a later study, the same researchers postulated that these new crystals grow around the inorganic fillers and that specific interactions result in a strong adhesion between polymer and fillers.[31] Even though no melting transition could be observed at such high temperatures in the present study, a similar effect was observed relating the enthalpies at the two endothermic transitions presented above.

CONCLUSIONS

The combination of Q-MMT and EPVOH resulted in the lowest overall water vapor permeability at 80% RH (<1.0 g/Pa·s·m x 10^{-5}) at low filler additions, thus demonstrating a positive effect of the organophilic Q-MMT clay in reducing the water sensitivity of the polymer. Annealing the EPVOH film at 120°C for 10 minutes led to a reduction in OP by a factor of 1.5. Annealed composite films containing 3 pph filler led to OP values at or below 1.0 $cm^3 \cdot cm/m^2 \cdot d \cdot bar$, or a reduced OP by a factor of 2.1-2.5 compared to the non-annealed films. Hence, the combined impact of filler addition and annealing was found to promote an effective reduction in the oxygen permeability.

The clay layers act as physical cross-links and these cross-links may reduce swelling and hinder dissolution of the composite films in water. Higher resistance to dissolution in water for composites containing Na-MMT, both for films dried at 23°C and annealed films were observed, which may be ascribed to stronger interactions between the clay and the polymer, due to matching polarities.

ACKNOWLEDGEMENTS

The authors would like to acknowledge Professor Chris Breen for valuable comments on this manuscript.

REFERENCES

1. Leonard, M.W. Barrier and overprint coatings. In The Wiley Encyclopedia of Packaging Technology, 3rd ed.; Yam, KL., Ed.; John Wiley & Sons Inc., **2009**; pp 98-103.
2. Foster, R.H. Ethylene-vinyl alcohol copolymers. In The Wiley Encyclopedia of Packaging Technology, 3rd ed. ; Yam, KL., Ed.; John Wiley & Sons Inc., **2009**; pp 418-423.

3. Ashley, R.H. Permeability and plastic packaging. In Polymer Permeability; Comyn, J., Ed.; Elsevier Applied Science Publishers: Essex, UK, **1985**; pp 269-308.
4. Weilbacher, R. Polyvinyl alcohol and modified polyvinyl alcohols for barrier coatings, In Kleebauer, M. and Sangl, R., Eds; PTS Workshop Innovative Packaging, GV 773, PTS, Munich, 2007; 6-1.
5. Johansson, C. and Clegg, F. (2014) Hydrophobically modified poly(vinyl alcohol) and bentonite nanocomposites thereof: Barrier, mechanical and aesthetic properties. Accepted for publication in *J. Appl. Polym. Sci.*
6. Alexandre, M. and Dubois, P. Polymer-layered silicate nanocomposites: preparation, properties and uses of a new class of materials. *Mater. Sci. Eng.* **2000**, *28*, 1-63.
7. Bharadwaj, R.K. Modeling the barrier properties of polymer-layered silicate nanocomposites. *Macromolecules* **2001**, *34*, 9189-9192.
8. McGlashan, S.A. and Halley, P.J. Preparation and characterization of biodegradable starch-based nanocomposite materials. *Polymer Int*. **2003,** *52*, 1767-1773.
9. Xie, F., Halley, P.J. and Avérous, L. Bio-nanocomposites based on starch. In Nanocomposites with biodegradable polymers. Synthesis, properties and future perspectives; Mittal V., Ed.; Oxford University Press: Oxford UK, **2011**; pp 234-260.
10. LeBaron, P.C., Wang, Z. and Pinnavaia, T.J. Polymer-layered silicate nanocomposites: an overview. *Appl. Clay Sci*. **1999,** *15*, 11-29.
11. Mittal, V. Bio-nanocomposites: future high-value materials. In Nanocomposites with biodegradable polymers. Synthesis, properties and future perspectives; Mittal, V., Ed.; Oxford University Press: Oxford UK, **2011**; pp 1-27.
12. Park, H.M., Li, X., Jin, C.Z., Park, C.Y., Cho, W.J. and Ha, C.H. Preparation and properties of biodegradable thermoplastic starch/clay hybrids. *Macromol. Mater. Eng*. **2002**, *287(8)*, 553-558.
13. Sinha Ray, S. and Bousmina, M. Biodegradable polymers and their layered silicate nanocomposites: In greening the 21st century materials world. *Prog. Mater. Sci*. **2005**; *50*, 962-1079.
14. Carrado, K.A., Thyagarajan, P., Elder, D.W. Polyvinyl alcohol-clay complexes formed by direct synthesis. *Clays Clay Miner*. **1996,** *44(4)*, 506-514.
15. Chen, B., Evans, J.R.G. Thermoplastic starch-clay nanocomposites and their characteristics. *Carbohydr. Polym*. **2005**, *61*, 455-463.
16. Paul, M.A., Alexandre, M., Degée, P., Henrist, C., Rulmont, A. and Dubois P. New nanocomposite materials based on plasticized poly(L-lactide) and organo-modified montmorillonites: thermal and morphological study. *Polymer* **2003**, *44*, 443-450.
17. Toyoshima K. Properties of polyvinyl alcohol films. In Polyvinyl alcohol Properties and Applications; Finch, C.A., Ed.; John Wiley & Sons Ltd. **1973**; pp 339-389.
18. Assender, H.E. and Windle, A.H. Crystallinity in poly(vinyl alcohol). 1. An X-ray diffraction study of atactic PVOH. *Polymer* **1998,** *39(18)*, 4295-4302.
19. Vaia, R.A. In Pinnavaia, TJ, Beall GW (eds). *Polymer-clay nanocomposites*. John Wiley and Sons: Chichester, England, **2000**; pp 245-249.
20. Breen, A.F., Breen, C., Clegg, F., Döppers, L.M., Khairuddin, Labet, M., Sammon, C., Yarwood, J. FTIR-ATR studies of the sorption and diffusion of acetone:water mixtures in poly(vinyl alcohol)-clay nanocomposites. *Polymer* **2012,** *53*, 4420-4428.

21. Khairuddin. Clay-polyvinylalcohol nanocomposites: competitive adsorption of polyvinylalcohol and plasticizers onto Na-bentonite. Ph.D. Thesis. Awarding Body: Sheffield Hallam University, 2012.
22. Mansur, H., Sadahira, C.M., Souza, A.N. and Mansur, A.A.P. FTIR spectroscopy characterization of poly(vinyl alcohol) hydrogel with different hydrolysis degree and chemically crosslinked with glutaraldehyde. *Mater. Sci. Eng*.: C. **2008**, *28*, 539-548.
23. Katti, K. and Katti, D.R. Relationship of swelling and swelling pressure on silica-water interactions in montmorillonite. *Langmuir* **2006**, *22*, 532-537.
24. Thomas, P.S. and Stuart, B.H. A Fourier transform Raman spectroscopy study of water sorption by poly(vinyl alcohol). *Spectrochimica Acta Part A* **1997**, *53*, 2275-2278.
25. Hodge, R.M., Edward, G. and Simon, G.P. Water absorption and states of water in semicrystalline poly(vinyl alcohol) films. *Polymer* **1996**, *37(8)*, 1371-1376.
26. Nazarenko, S., Meneghetti, P., Julmon, P., Olson, B.G and Qutubuddin, S. Gas barrier properties of polystyrene montmorillonite clay nanocomposites: effect of mineral layer aggregation. *J. Polym. Sci. Part B: Polymer Physics* **2007**, *45*, 1733-1753.
27. Nakane, K., Yamashita,T., Iwakura, K. and Suzuki F. Properties and structure of poly(vinyl alcohol)/silica composites. *J. Appl. Polym. Sci*. **1999**, *74*, 133-138.
28. Hodge, R.M., Bastow, T.J., Edward, G.H., Simon, G.P. and Hill, A.J. Free volume and the mechanism of plasticization in water-swollen poly(vinyl alcohol). *Macromolecules* **1996**, *29*, 8137-8143.
29. Tubbs, R.K. and Wu, T.K. Thermal properties of polyvinyl alcohol. In Polyvinyl alcohol Properties and Applications; Finch, C.A. Ed.; John Wiley & Sons Ltd. **1973**; pp 167-181.
30. Mallapragada, S.K. and Peppas, N.A. Dissolution mechanism of semicrystalline poly(vinyl alcohol) in water. *J. Polym. Sci. Part B: Polymer Physics* **1996**; *34*, 1339-1346.
31. Strawhecker, K.E. and Manias, E. AFM of poly(vinyl alcohol) crystals next to an inorganic surface. *Macromolecules* **2001**, *34*, 8475-8482.
32. Zhu, L. and Wool, R.P. Nanoclay reinforced bio-based elastomers: Synthesis and characterization. *Polymer* **2006**, *47*, 8106-8115.
33. Strawhecker, K.E. and Manias, E. Structure and properties of poly(vinyl alcohol)/Na^+ montmorillonite nanocomposites. *Chem. Mater*. **2000**, *12*, 2943-2949.

SUPPLEMENTARY MATERIAL

Moisture content at equilibrium and moisture uptake at different relative humidity

The equilibrium moisture content (Equation (1)) of PVOH and EPVOH films stored at 23°C and 50% RH was about 9.6% and 8.2%, respectively (Figure S1). Further moisture uptake of the PVOH and EPVOH films was achieved by exposing the films at consecutively higher RH in the climate chamber. The films were placed in the chamber allowing the moist air to freely circulate, ensuring that the RH was identical on both sides. The RH was increased from 50 to 90% RH at 10% intervals. The moisture uptake was recorded by weighing the samples after exposure for 24 h at each RH. The moisture uptake of films containing fillers were recorded in a similar way but at closer RH intervals, namely 70, 75, 80 and 85% RH.

The recorded moisture uptake in grams as well as in terms of calculated moisture content (from values pre-determined at 50% RH) as a function of increasing RH (Figure S1) show that both film types absorb increasing amounts of moisture, but the increase is slightly higher for PVOH, especially at RH $\geq$80%.

After annealing the reference PVOH films at 80, 100, 120 or 140°C for 10 minutes, followed by re-conditioning at 23°C and 50% RH for 24 h, the average moisture content was about 7%, independently of annealing temperature. This indicates that annealing for 10 min causes a 'permanent' reduction of the equilibrium moisture content of the films (a 2.6 percentage unit reduction). The EPVOH film annealed at 120°C for 10 minutes had a moisture content of 6.8% after re-conditioning (a 1.4% unit reduction). PVOH and EPVOH films dried at 105°C but for much longer time (90 min) both showed a moisture content around 0.6% after re-conditioning in 23°C and 50% RH for 24 h showing a much greater reduction than when treated for short time. Both PVOH and EPVOH films when exposed to 80% RH at 23°C for 24 hours, then dried at 105°C for 90 min followed by re-conditioning at 50% RH contained about 3.5% moisture, thereby confirming that extensive drying at relatively low temperatures and for long periods of time results in a permanent resistance to absorb moisture from the environment even for those films which have been exposed to high moisture environments.

The equilibrium moisture content determined by Equation (1) after exposing the films at 80% RH for 24 h was about 15.0 ± 0.4% for the PVOH film and 14.8 ± 0.1% for the EPVOH film (average from triplicates). This value is slightly higher than the corresponding calculated values of 11.2 and 10.0% from the recorded moisture uptake by step-wise exposure to increasingly higher RH (Figure S1). Thus, direct placement of the films in a high RH atmosphere seems to encourage a higher moisture uptake compared to successive exposure to small incremental changes up to the same RH level. Since the exposure time was 24 h at each specific RH (assumed sufficient to attain equilibrium), a step-wise increase from 50 to 60-70-80% RH provided the films with a longer total time to adjust to the higher RH environment, which could depress the amount of water uptake, particularly if there was an initial kinetic overshoot which then relaxed back to the equilibrium loading.

The moisture uptake curves in the films containing fillers in the relative humidity range 70-85% RH followed similar shape as the curves in Figure S1 (data not shown). A general trend towards reduced weight increase with increased filler content was found for all composite films. Expressed in normalized terms, i.e. moisture uptake for composite films with 12 pph filler relative to the EPVOH

film at the same relative humidity, the values were about 0.93-0.99 for Q-MMT, 0.85-0.90 for C-MMT and 0.68-0.75 for Na-MMT over the range 70-85% RH. It is thus evident that the EPVOH/Na-MMT nanocomposite film absorbed less moisture when exposed to moist atmosphere whereas the Q-MMT composite films followed the moisture uptake curve of the EPVOH more closely, thus representing the presence of more moisture in these films. The Na-MMT and C-MMT clays interact more intimately with the EPVOH (via hydrogen bonding) due to their similar polarities and water entering will thus have to compete to interact directly with the clay or EPVOH. This will limit the ability for water to penetrate the network and become adsorbed, thus leading to the reduced moisture content observed. The Q-MMT is inherently less prone to absorb water and does not interact with the EPVOH as strongly (as evidenced by XRD and FTIR); hence the polymer phase in this composite behaves in a similar manner to that of pure EPVOH.

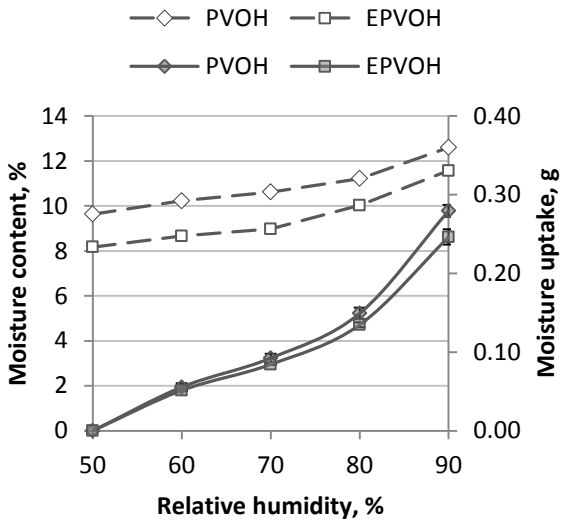

Figure S1. Measured moisture uptake of PVOH and EPVOH films (pre-conditioned at 23°C and 50% RH for 24 h) as average of duplicates with standard deviation (filled symbols) and calculated moisture content (open symbols) as a function of relative humidity.

Calculations for maximum uptake of non-freezable water for EPVOH

The maximum water uptake can be calculated by dividing the mass of one mole H_2O (18 g) by the sum of masses for one mole H_2O and one vinyl alcohol monomer unit (44 g), which equals to 29 wt%. This figure is valid also for the vinyl alcohol groups in EPVOH, but realizing that EPVOH contains fewer –OH groups for a given chain length compared to PVOH, as previously shown by NMR and M_w characterization[5], site saturation by absorption of water would be reached at a lower level. The molecular formula for EPVOH can be written $–[CH_2\text{-}CH(OCOCH_3)]_m– [CH_2\text{-}CH(OH)]_n–[CH_2\text{-}CH_2]_o–$ [4] where the suffixes *m* and *n* and *o* corresponds to the number of each unit. Using the data in Johansson and Clegg[5], the number *m* of vinyl acetate units are identical in polymer chains of equal length, i.e. 1-2 mol%, since the DH is equal in both PVOH and EPVOH. Substituting a number of vinyl alcohol groups (*n*-*o*) with a number of ethylene groups (*o*) corresponding to 8.1 mol% ethylene reduces the number of available sites (–OH groups) for water to attach. The degree of polymerization, P_W, of PVOH was calculated to 1595 based on the measured M_W[5] and the simple formula $P_W=M_W/(M_{VAc} \times 0.02+M_{VOH} \times 0.98)$ where M_{VAc} is the molecular weight of vinyl acetate (86 g/mol) and M_{VOH} is the molecular weight of vinyl alcohol (44 g/mol). Setting the number of vinyl

acetate units to 0.98 x 1595 gives 1563 units, i.e. 1563 available sites for attaching water molecules. This number is reduced to 1436 if replaced with 8.1 mol% ethylene. Hence, for an identical chain length, site saturation should be reached at about 26-27 wt%, which is reflected in the lower moisture uptake of EPVOH films observed in the annealed samples and those exposed to increasing humidity.

Dissolution in water

An initial immersion test with PVOH and EPVOH films in de-ionized water for short time (10 minutes) at room temperature demonstrated that both polymer types swell rapidly with an increase in film dimensions by ~40%. Ingress of water into the amorphous regions will cause the polymer to swell whereas dissolution requires break-up of the individual crystallites, i.e. replacement of intermolecular hydrogen bonds with polymer-water hydrogen bonds[18]. With immersion in deionized water for 36 h the fraction of dissolved matter (Equation (S1)) was found to strongly decrease with increased annealing temperature of PVOH, thus indicating that the degree of crystallinity increased upon annealing. Films annealed at 140°C showed a slight yellowing effect and so the annealing temperature for subsequent films containing EPVOH and fillers was limited to 120°C for 10 minutes.

The degree of water dissolution was measured by cutting film pieces ca. 20 x 30 mm which were weighed and placed in plastic tubes fitted with screwtops. Deionized water (50 ml) was added to each tube and the immersed film samples were allowed to stand at room temperature for 36 h. The water was then carefully poured off and the film pieces were dried at 105°C until constant weight, W_d. The fraction of dissolved matter was calculated by Equation (S1), taking the actual equilibrium moisture content already determined using Equation 1 into consideration:

$$Fraction\ dissolved\ matter = \frac{W_i - W_d}{W_i} x\ 100 \qquad \text{(S1)}$$

where W_i is the initial weight (W_0 x fraction of dry matter).

Hodge *et al*.[25] concluded that water dissolves poly(vinyl alcohol) crystallites at ambient temperature when present in excess quantities. With addition of increasing amount of water to dry PVOH, the maximum amount of non-freezing water in the amorphous region is reached and further addition results in free water. This additional water helps to separate the folded chains and delaminate the PVOH layers in crystallites. The crystallites dissolve gradually and eventually become totally swollen, i.e. a fully amorphous state is reached. Eventually, the PVOH molecules become completely disassociated from the crystal and then enter into transient hydrogen bonding with the PVOH chains in the previously crystalline region. Meanwhile near the surface of the water swollen PVOH - a now completely disentangled, free PVOH molecule (or indeed two or more loosely associated PVOH molecules) may diffuse into the bulk of the solvent. Hodge *et al*.[25] reported a saturation level of 60% total water content in PVOH films after 12 hours of immersion (present as free+bound water). Applying this explanation to the observations in the present study concerning EPVOH-clay composites, this latter step probably also involves withdrawal of filler particles since a portion of EPVOH chains are assumed to be adsorbed onto clay particles.

The fraction dissolved matter of pure EPVOH was only 48% as compared to 59% for the PVOH film when dried at 23°C and 50% RH. This demonstrates the higher resistance of the hydrophobic EPVOH to dissolve in water. In contrast, after annealing pure PVOH at 120 °C only 5% fractional dissolved

matter was observed, compared to 15% for EPVOH. This could suggest that less induced crystallinity occurs with EPVOH, presumably due to the presence of the ethylene groups within the polymer chains.

The fraction dissolved matter of EPVOH films containing fillers are depicted in Figure S2. The fraction dissolved matter was found to decrease with increased concentration of filler from 0 to 12 pph for films stored at 23°C/50% RH (filled symbols). The degree of dissolution decreased in the order Q-MMT>C-MMT>Na-MMT. Breen *et al*.[20] concluded that Na-MMT and PVOH are strongly bound and move in unison as the nanocomposite expands when water enters a PVOH-clay film. It is thus possible that the strong adsorption of the EPVOH polymer onto Na-MMT forms a robust network that prevents both polymeric and mineral species from leaching out into the water phase. EPVOH is anticipated to adsorb less strongly to Q-MMT and thus less likely to inhibit dissolution. The apparently lower tendency for EPVOH to adsorb on C-MMT compared to Na-MMT requires further attention.

A strong reduction in the fraction dissolved matter was found for all samples containing filler after annealing at 120 °C (open symbols). For C-MMT, a plateau level immediately below 10% was reached after addition of 3 pph clay. Q-MMT showed a similar trend (except for the point at 6 pph Q-MMT) and rather independent on the filler level. However, in case of Na-MMT, a continuous decrease in fraction dissolved matter was found up to 9 pph where a plateau level was reached.

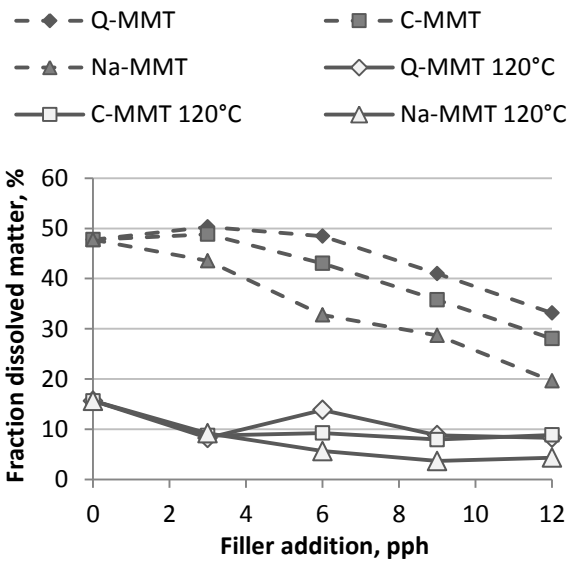

Figure S2. Fraction dissolved matter of EPVOH films as a function of filler addition. Dried at room temperature (filled symbols) with standard deviation ~6% and annealed at 120°C (open symbols) with standard deviation ~3%. Error bars hidden for clarity.